Electronic structures of efficient $M\mathrm{BiO_3}$ (M = Li, Na, K, Ag) photocatalyst*

Wen-Liu Zhou(周文流) and Zong-Yan Zhao(赵宗彦)†

Faculty of Materials Science and Engineering, Key Laboratory of Advanced Materials of Yunnan Province, Kunming University of Science and Technology, Kunming 650093, China

(Received 14 June 2015; revised manuscript received 11 November 2015; published online 18 January 2016)

In order to deepen the understanding of the relationship between fundamental properties (including: microstructure and composition) and photocatalytic performance, four bismuthate compounds, including: $LiBiO_3$, $NaBiO_3$, $KBiO_3$, and $AgBiO_3$, are regarded as research examples in the present work, because they have particular crystal structures and similar compositions. Using density functional theory calculations, their structural, electronic, and optical properties are investigated and compared systematically. First of all, the calculated results of crystal structures and optical properties are in agreement with available published experimental data. Based on the calculated results, it is found that the tunneled or layered micro-structural properties lead to the stronger interaction between bismuth and oxygen, and the weaker interaction between alkaline-earth metal and [BiO_6] octahedron, resulting in the feature of multi-band gaps in the cases of $LiBiO_3$, $NaBiO_3$, and $KBiO_3$. This conclusion is supported by the case of $AgBiO_3$, in which the feature of multi-band gaps disappears, due to the stronger interaction between the noble metal and [BiO_6] octahedron. These properties have significant advantages in the photocatalytic performance: absorbing low energy photons, rapidly transferring energy carriers. Furthermore, the features of electronic structures of bismuthate compounds are well reflected by the absorption spectra, which could be confirmed by experimental measurements in practice. Combined with the calculated results, it could be considered that the crystal structures and compositions of the photocatalyst determine the electronic structures and optical properties, and subsequently determine the corresponding photocatalytic performance. Thus, a novel Bi-based photocatalyst driven by visible-light could be designed by utilizing specific compositions to form favorable electronic structures or specific micro-structures to form a beneficial channel for energy carriers.

Keywords: bismuthate, photocatalysis, electronic structure, density functional theory calculations

PACS: 71.20.–b,71.20.Nr, 81.05.Hd, 82.20.Wt **DOI:** 10.1088/1674-1056/25/3/037102

1. Introduction

With rapid economy development, people are facing more and more severe challenges of energy shortage and environmental deterioration, which are becoming increasingly prominent and attract more and more attention. Photocatalysis technology can provide effective solutions to address these challenges.[1,2] At present, most research on photocatalysis focuses on the modifications for TiO_2,[3] because it is the prototype for the development of a novel photocatalyst. In the 1970s, Fujishima and Honda found electrochemical photolysis of water at the TiO_2 electrode under UV-light irradiation,[4] which opened a new era of heterogeneous photocatalysis. However, as a wide band gap (3.0–3.2 eV) semiconductor, TiO_2 only responds to UV-light, and thus its solar energy utilization efficiency is very low. At the same time, the photogenerated electron–hole pairs can recombine very easily, resulting in its low quantum conversion efficiency. Although researchers attempt to improve its photocatalytic performance by using modification methods (such as, impurity doping, noble metal loading, hetero-structure constructing, and dye sanitizing, etc.),[5,6] it is difficult for its performance to achieve the requirements of industrialized application in the short term. Therefore, to develop a novel efficient photocatalyst driven by visible-light is a major trend in the recent research of photocatalysis.

In recent years, the Bi-based photocatalyst has attracted wide attention because of the interesting photocatalytic performance under visible-light irradiation, and the diversity and flexibility of its structures and properties. It has been found that many Bi-based compound semiconductors have narrow band gaps and present efficient photocatalytic activity, resulting from the hybridized valence band between O-2p states and Bi-6s states. These results indicated that Bi-based compounds and composites have become an important family of photocatalysts driven by visible-light.[7–9] In particular, bismuthates ($M\mathrm{BiO_3}$) contain Bi^{5+} with 6s empty orbital, which contributes to both the top of the valence band and the bottom of the conduction band. This feature can vary the band edge positions and narrow the band gap, leading to the relatively high photocatalytic activity under visible-light irradiation.[10] For example, Ramachandran *et al.* evaluated the photocatalytic activity of $KBiO_3$ and $LiBiO_3$ for the degradation of anionic and cationic dyes under UV and solar radiations, and observed that the dye structure determines the effectiveness of photocat-

*Project supported by the National Natural Science Foundation of China (Grant No. 21473082).

†Corresponding author. E-mail: zzy@kmust.edu.cn

© 2016 Chinese Physical Society and IOP Publishing Ltd

alytic reactions.[11] $NaBiO_3$ also exhibits much higher activity compared with $BiVO_4$ and N-doped TiO_2 for the decomposition of methylene blue under visible light. Kako *et al.* considered that the attractive performance of $NaBiO_3$ is ascribed to its band structure where the CB consists of hybridized Na-3s and O-2p orbitals that exhibit large dispersion with high mobility for photo-excited electrons.[12]

Although bismuthates exhibit high photocatalytic activity, their fundamental photophysical properties have not been systematically studied and compared. In order to deepen the understanding of the relationship between fundamental properties (including: microstructure and composition) and photocatalytic performance, four bismuthate compounds MBiO$_3$ (M = Li, Na, K, Ag) are regarded as research examples in the present work, because they have particular crystal structures and similar compositions. (i) $LiBiO_3$ and $KBiO_3$ have tunneled structures, while $NaBiO_3$ and $AgBiO_3$ have layered structures. (ii) Li, Na, and K belong to the elements of alkaline-earth metals that have similar features. (iii) Although Na and Ag belong to different periodic table groups, $NaBiO_3$ and $AgBiO_3$ have the exact same crystal structure. In short, the similarities and differences between these four compounds have provided an opportunity to thoroughly investigate the relationship between the fundamental properties and the photocatalytic performance of bismuthates. The previous experimental observations about these MBiO$_3$ photocatalysts were independently reported by different research groups. Since their synthesis processing, experimental condition, and evaluation criteria are not completely consistent, so their experimental results cannot directly be compared to achieve this purpose. Different from the experimental study, the atomic-scale theoretical calculation can obtain comparable results for different materials based on the unified computational method and platform.[13–15] Hence, in this paper, we used density functional theory (DFT) to calculate the crystal structures, electronic structures, and optical properties of MBiO$_3$ (M = Li, Na, K, Ag). Based on the calculated results, the underlying photocatalytic mechanism of MBiO$_3$ and the corresponding photocatalytic performance are analyzed. Our calculated results would be used as a reference for the development of efficient Bi-based photocatalyst driven by visible-light using specific compositions to form favorable electronic structures or specific micro-structures to form a beneficial channel for energy carriers.

2. Computational methods

In the present work, the original crystal models are taken from the Inorganic Crystal Structure Database (ICSD). All of the DFT calculations were carried out by using Cambridge Serial Total Energy Package (CASTEP) codes that is interpolated in the package of Materials Studio 5.5,[16] which is a state-of-the-art quantum mechanics-based program designed specifically for solid-state materials science. According to the Born–Oppenheimer approximation and Hartree–Fock approximation, the core electrons (Bi: [Xe], O: [He], Li: [He], Na: [Ne], K: [Ar], Ag: [Kr]) were treated with the ultra soft pseudo-potential, while the exchange–correlation effects of valence electrons (Bi: $6s^26p^3$, O: $2s^22p^4$, Li: $1s^22s^1$, Na: $2s^22p^63s^1$, K: $3s^23p^64s^1$, Ag: $4d^{10}5s^1$) were described by the revised Perdew–Burke–Ernzerh for solid (PBEsol) of generalized gradient approximation (GGA).[17] It is well known that standard GGA method underestimates the band gap of semiconductor by $\sim 50\%$,[18] consequently the calculated results could not be compared with and confirmed by the experimental measurements directly. In order to overcome the shortcoming of GGA and obtain accurate electronic structures, the GGA+U method was adopted in the present work, and the values of $U_{\rm eff}$ were set as follows: 2 eV for the p states of Bi, Na, K, and O; 3 eV for Ag-d states. The values of $U_{\rm eff}$ are determined by the comparison between calculated band gaps and the corresponding experimental results, according to the repeated test. In the present work, we set the same values of $U_{\rm eff}$ for Bi and O in all compounds.

An energy cutoff of 380–410 eV was used to expand the Kohn–Sham wave functions. The Monkhorst–Pack scheme k-points grid sampling was set as $2\times3\times1$–$3\times3\times3$ for the irreducible Brillouin zone. A $40\times40\times40$–$60\times60\times60$ mesh was used for fast Fourier transformation. We use Broyden–Fletcher–Goldfarb–Shanno (BFGS) scheme[19] as the minimization algorithm, in which all atomic positions and lattice parameters are optimized. Its convergence criteria were set as follows: the force on the atoms was less than 0.01 eV/Å, the stress on the atoms was less than 0.02 GPa, the atomic displacement was less than 5×10^{-4} Å, and the energy change per atom was less than 5×10^{-6} eV. Based on the optimized crystal structures, the electronic structures and optical properties were then calculated.

3. Results and discussion

3.1. Crystal structures

Four crystal structures of bismuthates are illustrated in Fig. 1. The coordination numbers in these bismuthate compounds are 6 for Bi atoms, 2 for O atoms (in $AgBiO_3$, the coordination number of O is 3), 0 for Li (Na, K), and 3 for Ag atoms. $LiBiO_3$ has an orthorhombic structure with space group of Pccn (No. 56) and local symmetry D_{2h}^{10}; $NaBiO_3$ and $AgBiO_3$ have a trigonal structure with space group of $R\bar{3}$ (No. 148) and local symmetry C_{3i}^2; and $KBiO_3$ has a cubic structure with space group of $Pn\bar{3}$ (No. 201) and local symmetry T_h^2. It is known that their structure has rather regu-

lar or slightly distorted [BiO_6] octahedrons linked together at the corners and forming a network structure. In the cases of $LiBiO_3$ and $KBiO_3$, the octahedrons form a tunneled structure, and the alkaline-earth metals insert in the tunnels. In the cases of $NaBiO_3$ and $AgBiO_3$, the octahedrons form a layered structure, and Na atoms insert in the space between layers, the whole Ag atoms are bonded with oxygen atoms forming [AgO_3] tetrahedrons.

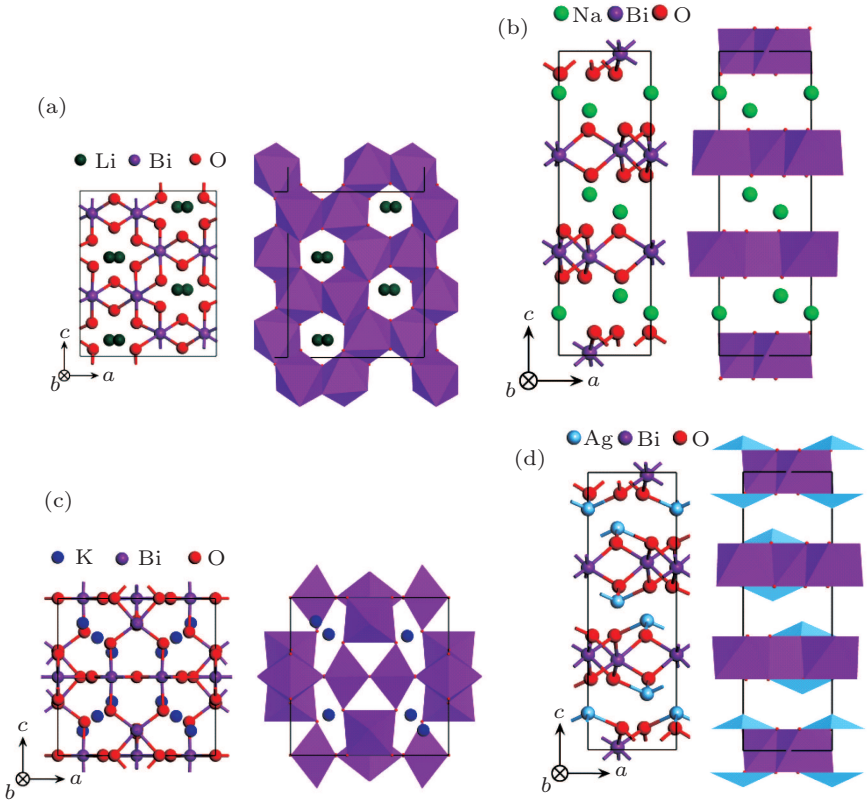


Fig. 1. (color online) The crystal structure models of four bismuthate compounds: (a) $LiBiO_3$, (b) $NaBiO_3$, (c) $KBiO_3$, and (d) $AgBiO_3$.

All the crystal lattice parameters for these four bismuthates are tabulated in Table 1, which are nicely consistent with experimental data,[20–22] indicating that the calculation methods in the present work are reasonable. Compared with the crystal structures of $NaBiO_3$ and $AgBiO_3$, one could find that their symmetries are identical, and the crystal structures are very similar. The main difference is the stronger interaction between Ag atoms and O atoms in $AgBiO_3$ than that in $NaBiO_3$, resulting in the Ag–O bond length (2.2974 Å) being shorter than the Na–O bond length (2.4608 Å). Hence, the lattice constants of $AgBiO_3$ are also slightly smaller than the lattice constants of $NaBiO_3$. For these four bismuthate compounds, the binding energy is decreasing with the increase of atomic number of M, which is calculated by the following equation: $E_B = -[E_{total} - \sum_i n_i E_i]/\sum_i n_i$ (where E_{total} is the total energy of bismuthate model, n_i and E_i are respectively the number and energy of a single atom in $15\times15\times15$ Å^3 box for the i atom in the bismuthate model). Resulting from the tunneled or layered structures, the decrease of binding energy implies that the interaction between [BiO_6] octahedron is weakening along with the increase of atomic number of M. For the application of photocatalysis, the tunneled and layered could improve the transfer behavior of photo-generated carriers. In particular, resulting from the small ionic radii of alkaline-earth metals, the ions of Li^+, Na^+, or K^+ maybe easily transfer in the tunnels or the space between layers. Thus, these ions could also carry the energy excited by the solar light. Although there is not alkaline-earth metal in $AgBiO_3$, the space between layers is large enough to allow the ions or radicals (such as H^+, OH^+, etc.) to transfer easily. Therefore, from the viewpoint of micro-structure, these bismuthates are potentially used as an efficient photocatalyst. Although this point is just a conjecture at the current stage, Wei *et al.* recently investigated the transport behavior of Li-ion in layered cathode materials (the kinetics of Li-ion diffusion versus selection of the advantageous paths, and their effective diffusion barriers depended on activation energies and Li-slab space) by using DFT calculations, and clarified how these factors tune the kinetics of Li diffusion in a delithiation process.[23] This published work provides great inspiration to us. In this paper, we research the transport behavior of the ions in $MBiO_3$ by using similar research ideas.

Table 1. The lattice constants and parameters, and the atomic average net charge from Mulliken population analysis of bismuthate compounds.

	$LiBiO_3$	$NaBiO_3$	$KBiO_3$	$AgBiO_3$
Symmetry	orthorhombic *Pccn* (D_{2h}^{10}, No. 56)	trigonal $R\bar{3}(C_{3i}^{2}$, No. 148)	cubic $Pn\bar{3}(T_h^2$, No. 201)	trigonal $R\bar{3}(C_{3i}^{2}$, No. 148)
Lattice constant (cal.)	$a = 8.9007$ Å, $b = 4.9615$ Å, $c = 10.8220$ Å $\alpha = \beta = \gamma = 90°$	$a = b = 5.6122$ Å, $c = 16.0733$ Å $\alpha = \beta = 90°$, $\gamma = 120°$	$a = b = c = 10.0432$ Å $\alpha = \beta = \gamma = 90°$	$a = b = 5.7038$ Å, $c = 15.5061$ Å, $\alpha = \beta = 90°$, $\gamma = 120°$
Lattice constant (exp.)[a]	$a = 8.8278$ Å, $b = 4.9135$ Å, $c = 10.6914$ Å $\alpha = \beta = \gamma = 90°$	$a = b = 5.6572$ Å, $c = 15.9890$ Å $\alpha = \beta = 90°$, $\gamma = 120°$	$a = b = c = 10.0194$ Å $\alpha = \beta = \gamma = 90°$	$a = b = 5.6411$ Å, $c = 16.118$ Å, $\alpha = \beta = 90°$, $\gamma = 120°$
Crystal volume /molecule·Å^3	59.7394	73.0715	84.4192	72.8125
Density /g·cm^{-3}	7.3360	6.3622	5.8239	8.3205
Binding energy /eV·atom^{-1}	5.7936	5.6910	5.5921	5.4276
Average bond length/Å	Li–O: 2.0018 Bi–O: 2.1345	Na–O: 2.4608 Bi–O: 2.1370	K–O: 2.6887 Bi–O: 2.1347	Ag–O: 2.2974 Bi–O: 2.1679
Average net charge/*e*	Li: 0.84 Bi: 1.96 O: –0.94	Na: 0.43 Bi: 2.05 O: –0.82	K: 0.28 Bi: 0.64 O: –0.31	Ag: 0.32 Bi: 1.97 O: –0.76

[a]Refs. [20]–[22].

3.2. Electronic structure

The band structures of these four bismuthates are illustrated in Fig. 2. In the present work, we found that the spin-up states and the spin-down states are completely coincident, owing to the pairing electrons in these four bismuthate compounds. For $LiBiO_3$, the valence band maximum (VBM) is located at the *k*-point line of $\Gamma \rightarrow Z$, while the conduction band minimum (CBM) is located at the Γ *k*-point, which means that $LiBiO_3$ is an indirect band gap semiconductor. The calculated band gap, the distance between VBM and CBM, is 1.7 eV, which is highly consistent with the experimental measurement ($E_g = \sim 1.8$ eV).[11] The band gap of $NaBiO_3$ (2.550 eV, which is highly consistent with the experimental measurement, 2.6 eV[24]) is larger than that of $LiBiO_3$, and also belongs to an indirect band gap semiconductor (the VBM is located at the *k*-point line of $F \rightarrow \Gamma$, while the CBM is located at the Γ *k*-point). In the case of $KBiO_3$, the VBM is located at the *M* *k*-point, while the CBM is located at the Γ *k*-point. Hence, the band gap of $KBiO_3$, 2.3 eV (which is strongly consistent with the experimental measurement, 2.1 eV[11]), belongs to the indirect band gap.

In the case of $AgBiO_3$, the highest VB and the lowest CB contact together, indicating that the minimum value of band gap is 0 eV. Above the lowest CB, one could see another forbidden band with an indirect pseudo-band gap of 2.563 eV, in which the pseudo-VBM/CBM is located at Γ/Z *k*-point. The band-gap value of $AgBiO_3$ is a very controversial issue. The sample color of $AgBiO_3$ is black,[25,26] implying its band gap is very small. Based on the UV–vis spectra, Takei *et al.* estimated its band gap is 0.87 eV,[26] while Yu *et al.* estimated its band gap is 2.5 eV.[27] On the contrary, using different calculation methods (linear muffin-tin orbital method and discrete-variational $X\alpha$ molecular orbital method), Mizoguchi *et al.*[25] and Takei *et al.*[26] independently obtained the band gap of $AgBiO_3$ is 0 eV. Carefully comparing the experimental measurements with theoretical calculations, we considered that the band gap of $AgBiO_3$ should be determined as 0 eV, and the experimental measurements might come from the electron transition deviated from Γ *k*-point or the electron transition between pseudo-VBM and pseudo-CBM in the second forbidden band.

The parameters of band structures of these four bismuthate compounds are listed in Table 2. Firstly, the direct band gaps are slightly larger than the minimum band gaps. This situation leads to difficult or certain confusion in the band gap measurement in practice. Importantly, the band structures of these four bismuthate compounds present the feature of multi-band gaps. In other words, their bands near the fundamental band gap are located and separated, which may be caused by the tunneled or layered structures. As shown in Table 2, the alkaline-earth metal's ns states are located below the valence band (VB) with a large band gap and a small band width. At the same time, the bands related to O-2s states and Bi-6s states are also below VB with relative small band gaps. These bands are not influenced by the extra-situation, and belong to the inner-energy bands. Therefore, they have an insignificant effect on the photocatalytic performance, and are not displayed in Figs. 1 and 2. These four bismuthate compounds have wide VBs with band widths > 4.2 eV, and the VB band width of $AgBiO_3$ is the largest. The conduction bands (CBs) of these four bismuthate compounds have two distinct parts: lower conduction band (CB_L) and upper

conduction band (CB_U), which are separated by > 2.1 eV. In the case of $KBiO_3$, the CB is divided into three distinct parts: CB_{L1}, CB_{L2}, and CB_U. Resulting from the identical crystal structure, the band structure of $AgBiO_3$ has similar features to that of $NaBiO_3$. However, because of the bonding between O atoms and Ag atoms (i.e., the strong interaction between O atoms and Ag atoms), the CB_L is noticeably down-shifting to the top of VB, leading to the zero band gap of E_{g1}. In other words, $AgBiO_3$ exhibits semi-metallic features. However, the CB_L contains only two energy levels, so this feature is not very prominent in the experimental measurement, and therefore has not attracted much attention in practice (see the discussion of optical properties in subsection 3.3). In the previous experimental works carried out by Takei *et al.*,[26] it was observed that only adsorption of methylene blue occurs on the $AgBiO_3$ and its photocatalytic activity for methylene blue decomposition is very low. However, Yu *et al.* found that $AgBiO_3$ has a superior inhibitory effect on the cyanobacteria at relatively low concentrations with natural light, causing irreversible damage to M. aeruginosa, compared with $AgNO_3$ and $NaBiO_3$.[27] Combining their UV–vis diffuse reflectance absorption measurement, we considered that this effect might be caused by the photo-generated electron–hole pairs on the VB, CB_L, and CB_U. Thereby, we suggest that the relationship between the semi-metallic properties and photocatalytic performance of the novel photocatalyst is very worthy of further investigation.

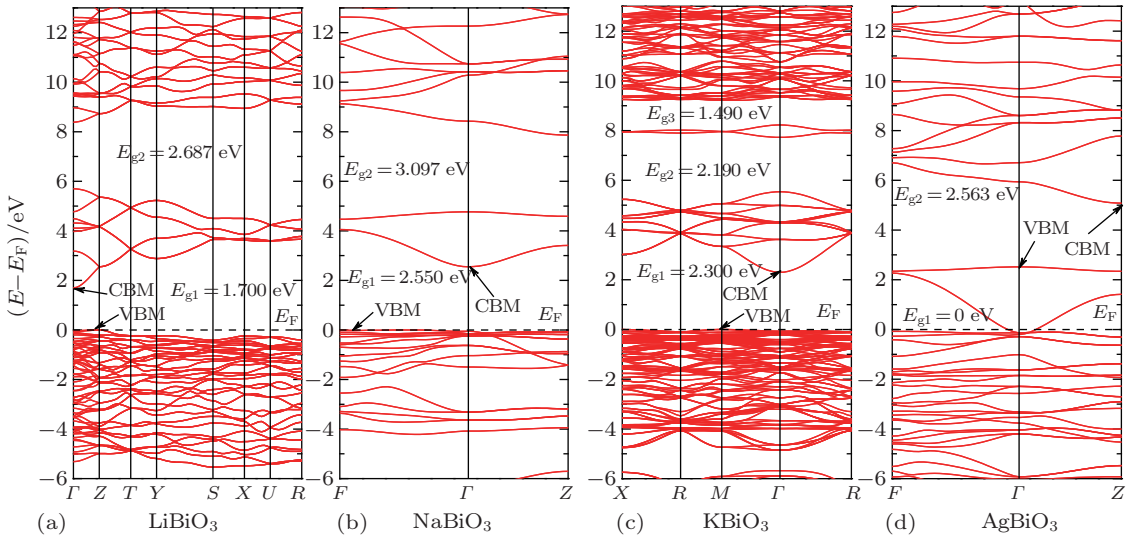


Fig. 2. (color online) The calculated band structures of four bismuthate compounds. (a) $LiBiO_3$, (b) $NaBiO_3$, (c) $KBiO_3$, and (d) $AgBiO_3$.

Table 2. The parameters of band structures of bismuthate compounds, the energy unit is eV.

		$LiBiO_3$	$NaBiO_3$	$KBiO_3$	$AgBiO_3$
Top of VB		$\Gamma \rightarrow Z$	$F \rightarrow \Gamma$	M	Γ
Bottom of CB		Γ	Γ	Γ	Γ
E_g (minimum)/eV[a]		1.70, 2.687	2.55, 3.097	2.30, 2.19, 1.49	0, 2.563
E_g (direct at Γ)/eV		1.740	2.613	2.373	0
Band gaps/eV		Li-s $\rightarrow$ O-2s: 22.863 O-2s $\rightarrow$ Bi-6s: 1.623 Bi-6s $\rightarrow$ VB: 0.657 $CB_L \rightarrow CB_U$: 2.687	Na-2s $\rightarrow$ O-2s: 1.401 O-2s$\rightarrow$ Bi-6s: 3.260 Bi-6s $\rightarrow$ VB: 1.689 $CB_L \rightarrow CB_U$: 3.097	K-3s $\rightarrow$ O-2s: 8.211 O-2s $\rightarrow$ Bi-6s: 3.261 Bi-6s $\rightarrow$ VB: 1.033 $CB_{L1} \rightarrow CB_{L2}$: 2.190 $CB_{L2} \rightarrow CB_U$: 1.490	O-2s $\rightarrow$ Bi-6s: 3.605 Bi-6s $\rightarrow$ VB: 1.433 VB $\rightarrow CB_L$: 0 $CB_L \rightarrow CB_U$: 2.563
Band width/eV	M-ns	0.028	0.011	0.727	5.709
	O-2s	3.115	3.233	3.295	2.798
	Bi-6s	4.425	3.775	2.885	3.305
	VB	5.536	4.2160	4.857	6.378
	CB_L	3.999	2.216	0.496, 3.240,	2.653
	CB_U	11.838	10.867	6.157	12.090

[a]The multi-band gaps of $MBiO_3$ are provided as the orders of first, second, and third band gaps as shown in Fig. 2.

To analyze the chemical bonding information, the total and partial density of states (DOS) of these four bismuthate compounds are plotted and compared in Fig. 3, which are highly consistent with the calculated results by discrete-variational $X\alpha$ molecular orbital method.[26] In general, the peaks and features of DOS for these compounds exhibit obvious similarity: (i) a deep band consists of Li(Na, K)-*n*s and O-2s, Bi-6s states; (ii) the lower VB is dominated by the hybridized states of O-2p and Bi-6p states; (iii) the middle and top of VB is dominated by the O-2p nonbonding states; (iv) the CB_L is mainly contributed by the hybridization states of O-2p and Bi-6s states; (v) the CB_U is mainly contributed by the Bi-6p states. In addition to the similarities mentioned above, due to the different crystal structures and compositions, these compounds also show some differences: (i) the K-3s states form the second lower conduction band (CB_{L2}) in the case of $KBiO_3$; (ii) due to the strong interaction between O atoms and Ag atoms in the case of $AgBiO_3$, the Ag-5s states also contribute to the form of VB hybridized with O-2p states, and the Ag-4d states also contribute to the form of CB_U. Because the Fermi energy level (E_F) is fixed at 0 eV in standard DFT calculations, so the band relative-shifting could be directly observed.

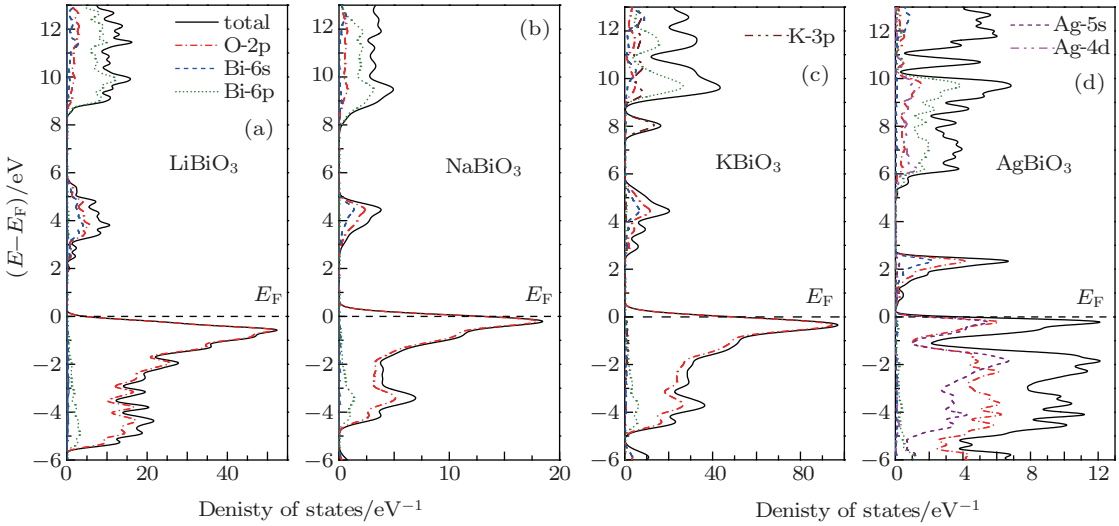


Fig. 3. (color online) The calculated density of states of four bismuthate compounds. (a) $LiBiO_3$, (b) $NaBiO_3$, (c) $KBiO_3$, and (d) $AgBiO_3$.

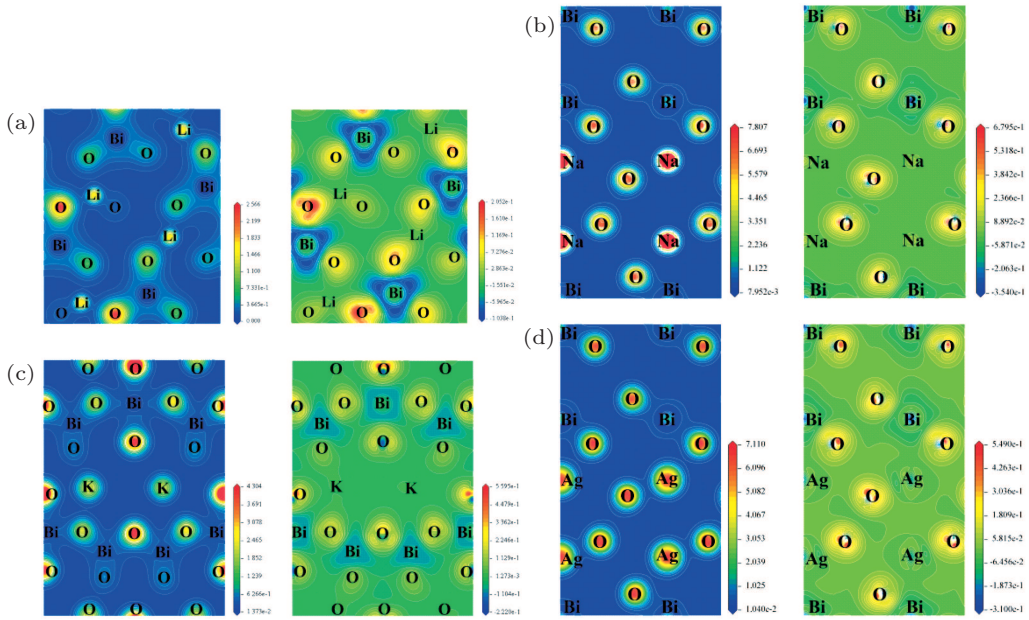


Fig. 4. (color online) The calculated contour maps of electron densities (right) and electron difference densities (left) of four bismuthate compounds. (a) $LiBiO_3$, (b) $NaBiO_3$, (c) $KBiO_3$, and (d) $AgBiO_3$.

The contour maps of electron densities and electron difference densities of these four bismuthate compounds are plotted and compared in Fig. 4. The characteristics of tunneled or layered structures are well presented in these maps. In the case of $LiBiO_3$, the electron densities and electron transfer are different around Li atoms and Bi atoms. The covalent bonds between Bi atoms and O atoms are stronger than those bonds between Li atoms and O atoms, and more electrons gather onto Bi–O bonds. By Mulliken population's analysis, the average net charge of Bi is 1.96*e*, which is larger than that of Li (0.84*e*). In the case of $NaBiO_3$, the bonds between Bi atoms and O atoms exhibit the feature of covalent bond, while the bonds between Na atoms and O atoms exhibit the feature of ionic bond. The interaction between atoms is obviously weaker than that in $LiBiO_3$, so the average net charge of Bi (2.05*e*) is the largest in these compounds. In the case of $KBiO_3$, the situation is similar to that of $NaBiO_3$. However, the average net charge on atoms is very small: 0.28*e* for K, 0.64*e* for Bi, and −0.31*e* for O, which are the smallest in these compounds. This calculated result indicates that the interactions between atoms in $KBiO_3$ are very weak. In the case of $AgBiO_3$, the bonding characteristics between Bi atoms and O atoms are very similar to those in $NaBiO_3$, and the layered feature is still clearly presented. But the bonding characteristics between Ag atoms and O atoms are different from those between Na atoms and O atoms in $NaBiO_3$: the Ag–O bonds exhibit an obvious feature of covalent bond. These characteristics of bonding information in the four bismuthate compounds indicate that the crystal structure and composition could determine the electronic structure, and subsequently determine the corresponding photocatalytic performance.

3.3. Optical properties

Figure 5 illustrates the calculated absorption spectra of four bismuthate compounds by the polycrystalline model. The optical properties of bismuthate compounds are determined by their compositions, crystal structures, and electronic structures. In turn, the differences of optical properties between these four bismuthate compounds could reflect the subtle differences among their crystal structures and electronic structures. Owing to the feature of multi-band gaps, when electrons on the top of VB absorb the incident photon energy, there are three kinds of electron transition: VB→CB_L, CB_L →CB_U, and VB→CB_U. In these absorption spectra, we could identify the absorption peak centered at 450–600 nm arising from the electron transition between the top of VB to the bottom of CB_L, and the absorption peak centered at 250–300 nm arising from the electron transition between the top of VB to the top of CB_U. This is because the CB_L is an unoccupied band above the Fermi energy level, and in the current first-principles only the electron transition between occupied states and unoccupied states is considered. Therefore, the absorption peak corresponding to the electron transition of CB_L →CB_U and VB→CB_L →CB_U is not calculated. Specifically, in the case of $AgBiO_3$, because the zero band gap of E_{g1} arising from CB_L connects the top of VB, the optical absorption in the visible-light region is very significant, which means that the electrons on the top of VB can be easily excited by lower photon energy.

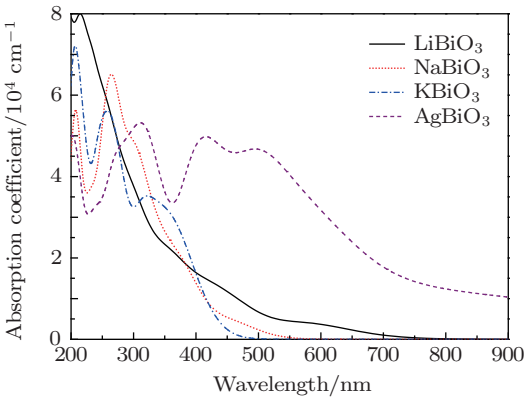


Fig. 5. (color online) The calculated absorption spectra of four bismuthate compounds by polycrystalline models.

However the absorption spectra calculated by DFT calculations are different from the experimental results, for example in the case of $AgBiO_3$. The differences may be because only a straightforward transition from occupied energy bands (VB) to unoccupied energy bands (CB_L and CB_U) is considered in DFT calculations, while in practice, owing to the semimetallic features, the electron transition from CB_L to CB_U could occur. However, their underlying mechanisms are identical to that determined by the electron transfer from the occupied energy bands to the unoccupied energy bands by photon excitation. Taking the experimental literature Ref. [27] as an example, the authors determined the optical band gap, based on the absorption edge in the range of 400–600 nm, which is corresponding to the electron transition from VB→CB_U in Fig. 2. However, in their absorption spectra, one could see that there are other shoulder absorption peaks in the visible-light region, which are contributed by the electron transition of CB_L →CB_U and VB→CB_L →CB_U. That is to say, the absorption spectra calculated here are good reflections of the multi-band-gap characteristics of these four bismuthate compounds.

4. Conclusions

The crystal structures, electronic structures, and optical properties of four bismuthate compounds (including: $LiBiO_3$, $NaBiO_3$, $KBiO_3$, and $AgBiO_3$) have been calculated by density functional theory. $LiBiO_3$ and $KBiO_3$ have tunneled structures, and $NaBiO_3$ has a layered structure. Thus, Li^+, Na^+, or K^+ ions may easily transfer in the tunnel or the layer space to

carry the solar energy, owing to the small ionic radii and the weak interaction with $[BiO_6]$ octahedrons. Although $AgBiO_3$ has an identical layered structure to $NaBiO_3$, the strong interaction between Ag atoms and O atoms, and the large radius of Ag^+, result in the Ag^+ ions being unable to transfer freely and form $[AgO_3]$ tetrahedron. The tunneled and layered micro-structures make these four bismuthate compounds have multi-band gaps, namely their bands near the fundamental band gap are located and separated. Also, these features of electronic structure are reflected by the absorption spectra, which could be confirmed by the experimental measurements. Based on the calculated results, it could be considered that the crystal structures and compositions of photocatalyst determine the electronic structures and optical properties, and subsequently determine the corresponding photocatalytic performance. Furthermore, the present work also presents some open issues that are worthy of in-depth investigation, such as: the transfer behavior of ions with small radii in the tunneled or layered photocatalyst, and the effects of the semi-metallic feature on photocatalytic performance.

References

[1] Schultz D M and Yoon T P 2014 *Science* **343** 1239176

[2] Valdes A, Brillet J, Gratzel M, Gudmundsdottir H, Hansen H A, Jonsson H, Klupfel P, Kroes G J, Le Formal F, Man I C, Martins R S, Norskov J K, Rossmeisl J, Sivula K, Vojvodic A and Zach M 2012 *Phys. Chem. Chem. Phys.* **14** 49

[3] Kamat P V 2012 *J. Phys. Chem. C* **116** 11849

[4] Fujishima A and Honda K 1972 *Nature* **238** 37

[5] Schneider J, Matsuoka M, Takeuchi M, Zhang J, Horiuchi Y, Anpo M and Bahnemann D W 2014 *Chem. Rev.* **114** 9919

[6] Chen X and Mao S S 2007 *Chem. Rev.* **107** 2891

[7] Blasse G, Dirksen G J and de Korte P H M 1981 *Mater. Res. Bull.* **16** 991

[8] Zhao Z, Li Z and Zou Z 2011 *Phys. Chem. Chem. Phys.* **13** 4746

[9] He R A, Cao S, Zhou P and Yu J 2014 *Chin. J. Catalysis* **35** 989

[10] Liu J, Chen S, Liu Q, Zhu Y and Zhang J 2013 *Chem. Phys. Lett.* **572** 101

[11] Ramachandran R, Sathiya M, Ramesha K, Prakash A S, Madras G and Shukla A K 2011 *J. Chem. Sci.* **123** 517

[12] Kako T, Zou Z, Katagiri M and Ye J 2007 *Chem. Mater.* **19** 198

[13] Zheng H M, Fang X Y, Cai L X, Yin A C, Jin H B, Yu X X and Cao M S 2014 *Chin. Phys. B* **23** 126102

[14] Yu Z Q, Xu Z M and Wu X H 2014 *Chin. Phys. B* **23** 107102

[15] Zhao Z Y, Yi J and Zhou D C 2014 *Chin. Phys. B* **23** 017401

[16] Clark S J, Segall M D, Pickard C J, Hasnip P J, Probert M J, Refson K and Payne M C 2005 *Z. Kristallogr.* **220** 567

[17] Perdew J P, Ruzsinszky A, Csonka G I, Vydrov O A, Scuseria G E, Constantin L A, Zhou X and Burke K 2008 *Phys. Rev. Lett.* **100** 136406

[18] Anisimov V I, Zaanen J and Andersen O K 1991 *Phys. Rev. B* **44** 943

[19] Pfrommer B G, Câté M, Louie S G and Cohen M L 1997 *J. Comput. Phys.* **131** 233

[20] Kumada N, Takahashi N, Kinomura N and Sleight A W 1996 *J. Solid State Chem.* **126** 121

[21] Kumada N, Kinomura N and Sleight A W 2000 *Mater. Res. Bull.* **35** 2397

[22] Nguyen T N, Giaquinta D M, Davis W M and zur Loye H C 1993 *Chem. Mater.* **5** 1273

[23] Wei Y, Zheng J, Cui S, Song X, Su Y, Deng W, Wu Z, Wang X, Wang W, Rao M, Lin Y, Wang C, Amine K and Pan F 2015 *J. Am. Chem. Soc.* **137** 8364

[24] Kako T, Zou Z, Katagiri M and Ye J 2007 *Chem. Mater.* **19** 198

[25] Mizoguchi H and Woodward P M 2004 *Chem. Mater.* **16** 5233

[26] Takei T, Haramoto R, Dong Q, Kumada N, Yonesaki Y, Kinomura N, Mano T, Nishimoto S, Kameshima Y and Miyake M 2011 *J. Solid State Chem.* **184** 2017

[27] Yu X, Zhou J, Wang Z and Cai W 2010 *J. Photoch. Photobio. B* **101** 265